JAST, Vol. 12, No. 2, pp. 35-48

JAST
Journal of Aerospace Science and Technology

Vibrational Characteristics of A Spinning Thermally Affected Cylindrical Shell Conveying Viscous Fluid Flow Carrying Spring-Mass Systems

A. R. Pourmoayed[1]*and K. Malekzadeh Fard[2]

1. Department of Mechanical Engineering, KhatmolAnbia Air Defense

2. Faculty of Structural Analysis and Simulation Centre, MalekAshtar University

* Basij Highway , Tehran, IRAN

Pourmoayed@mut.ac.ir

In this article, the vibrational behavior of a spinning cylindrical thick shell carrying spring-mass systems and conveying viscos fluid flow under various temperature distributions is investigated. This structure rotates about axial direction and the formulations include the coriolis and centrifugal effects. In addition, this system is conveying viscous fluid, and the related force is calculated by modified Navier –Stokes relation considering slip boundary condition and Knudsen number. The modeled cylindrical thick shell, its equations of motion, and boundary conditions are derived by the principle of minimum total potential energy and based on a new three-dimensional refined higher-order theory (RHOST). For the first time in the present study, attached mass-spring systems has been considered in the rotating cylindrical thick shells conveying viscous fluid flow. The accuracy of the presented model is verified with previous studies. The novelty of the current study is consideration of the rotation, various temperature distributions, mass-spring systems and conveying viscous fluid flow implemented on proposed model using RHOST. Generalized differential quadrature method (GDQM) is presented to discretize the model and to approximate the governing equations. In this study the simply supported conditions has been applied to edges $\theta = 0, 2\pi$ *and cantilever boundary conditions has been studied in x=0, L. Finally, the effects of the velocity of viscous fluid flow, angular velocity, temperature changes and spring-mass systems on the critical speed, critical velocity, critical temperature and natural frequency of the structure are investigated.*

Keywords: Various temperature distributions, Spring-mass systems, Cantilever cylindrical thick shell, Viscous fluid flow, Spinning

Introduction

Because of their good strength to weight ratio and simple manufacturing, cylindrical shell structures have attracted more attentions in comparison with other geometries in industry. Rotating cylindrical shell structures are the main parts of the various machines like jet engines, centrifugal separators, rockets, missiles, offshore drilling systems and spinning satellite structures. These structures tolerate various dynamic forces during their operating time which may affect on themselves and their equipment's efficiency. It means that, free vibration analysis of these structures has a key role in design and performance of these structures when they are subjected to dynamic excitations.

Observations show that history of dynamic analysis of rotating cylindrical shells returns to about a century ago. Bryan [1] was the first researcher who worked on rotating cylindrical shells by considering a rotating ring. He noticed the traveling mode phenomenon for the first time. Then, Taranto and Lesson[2] worked on the

rotating shells including coriolis effect. Next, Srinivasan and lauterbach[3] worked on traveling waves in infinite rotating cylindrical shells. Also Zohar and Aboudi [4] analyzed rotating finite thin cylinder.

Because of thin shell simplifying assumptions which neglects in plane inertia, transverse shear deformation and rotary inertia, the results are acceptable only for very thin shells and lower frequencies. In order to include the three-dimensional fully dynamic modeling of the cylindrical thick shell, researchers have usually used a high-order shear deformation theory (HSDT). pourmoayed et al [5] presented free vibration analysis of thick cylindrical shells with simply supported boundary conditions using improved HSDT. Khalili et al [6] investigated Free vibration analysis of homogeneous isotropic circular cylindrical shells based on a RHOST. In this article, the trapezoidal shape factor (1 +z/R) of a shell element is taken into account in the expressions of stresses to obtain the accurate stress-resultants over the thickness. In the field of rotating cylindrical thick shell, Jabbari et al [7] investigated thermo-elastic analysis of functionally graded (FG) rotating thick cylindrical pressure vessels with variable thickness subjected to the temperature gradient and internal non-uniform pressure. For the first time in this study, the effects of higher-order approximations on the radial and axial displacements, von Mises stress, and shear stress was studied. Nejad et al [8] presented elastic analysis of axially functionally graded rotating thick cylindrical shell with variable thickness under non-uniform arbitrarily pressure loading. In recently, Afshin et al [9] studied transient therm oelastic analysis of FGM rotating thick cylindrical pressure vessels under arbitrary boundary and initial conditions. All scopes of the above articles are dynamic analysis of rotating cylindrical shell structures but it should be noted that none of them have considered the rotating cylindrical shell conveying viscous fluid flow.

Firouz- abadi et al [10] presented a fluid–structure interaction model for stability analysis of shells conveying fluid. This model is applied to catch the eigenvalues and flow modes, which are used for the modal representation of the flow field in the cylindrical shell. Bochkarev et al [11] investigated, the stability of a rotating cylindrical shells interacting with a rotating internal fluid flow. They in this work showed, the form of stability loss in the stationary and rotating shells under the action of the fluid flow, having both the axial and circumferential components, depends on the type of the boundary conditions specified at their ends. Dynamic Stability/instability analysis of circular cylindrical shells with cantilever boundary conditions subjected to axial internal flow is presented by paak et al [12].

Recently, Rabani et al [13] studied, dynamic stability/instability and nonlinear vibration analysis of embedded temperature-dependent cylindrical shell conveying viscous fluid resting on temperature-dependent orthotropic Pasternak medium. They in this article, the effects of such parameters, on dynamic stability/instability of the cylindrical shell conveying viscous fluid presented.

In the field of cylindrical shell structures under thermal loadings, thermal and mechanical buckling of cylindrical FGM shells under the effect of geometrical imperfections with different types of loadings (Refs [14]; Mirzavand et al.[15]; Mirzavand and Eslami, [16]; Huang and Han, [17]) were presented. Their results demonstrate that the critical temperature difference for the cylindrical shell under nonlinear temperature changes is greater than that under linear temperature changes through the thickness. Banerjee [18] studied the vibrational behavior of beams carrying spring-mass systems. He used the dynamic stiffness method in order to analyze the beam. Numerical examples were given for a cantilever beam carrying a spring-mass at the tip. Recently, Hozhabrossadti et al [19] analyzed a beam with intermediate sliding connection joined by a mass-spring system. Also in other work, Hozhabrossadti et al [20] presented the free vibration analysis of a two-member grid coupled with a mass-spring system. Furthermore, an Euler Bernoulli beam carrying a lumped rotary inertial-rotational spring was investigated by Hozhabrossadati et al [21].

It is worth mentioning none of the previous works have considered viscous fluid flow and thermal loading on a rotary cylindrical thick shell with a mass-spring system using RHOST. The novelty of the current study is consideration of rotation, various temperature distributions, attached mass-spring systems and conveying viscous flow implemented on proposed model using RHOST.

Because of high accuracy and efficiency of the generalized differential quadrature method (GDQM), it is employed to solve the governing

equations of the problem. The governing equations and boundary conditions have been developed using Hamilton principle which are solved with the aid of the GDQM. Finally, in the results section show that, velocity of viscous fluid flow, angular velocity, temperature changes and spring-mass systems play an important role on critical speed, critical velocity, critical temperature and natural frequency of the structure.

Mathematical modeling

In Fig (1), a schematic spinning cylindrical shell conveying viscos fluid flow is presented. The length, the radius and the thickness of the shell denote with L, R and h, respectively. Moreover, Fig (2) presents a schematic of cylindrical thick shell carrying spring- mass systems. The cylindrical shell in x=L/2 is surrounded by spring. In addition, the free end of the structure is joined by bush.

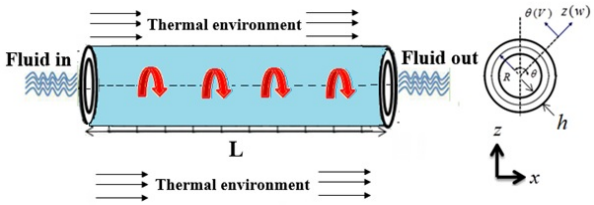

Figure 1. Geometry of a 3-D spinning cylindrical shell conveying viscos fluid flow in thermal environment.

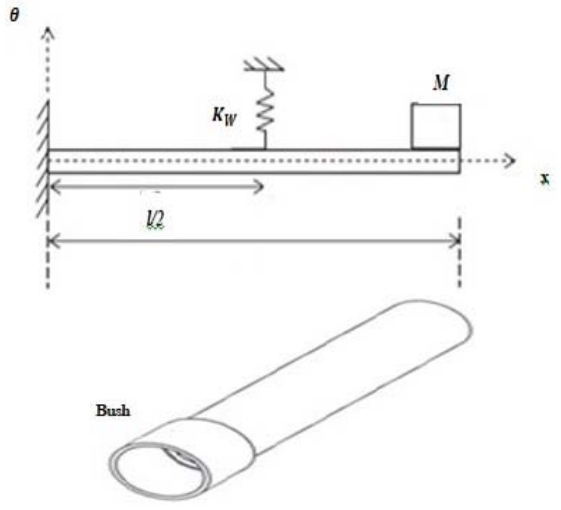

Figure 2. A cylindrical shell carrying spring- mass systems.

The mass of the bush is shown with M in the figure. The Taylor's series expansion is used to deduce a two-dimensional formulation of a three-dimensional elasticity problem and the following set of equations are obtained by expanding the displacement components $u(x,\theta,z)$, $v(x,\theta,z)$ and $w(x,\theta,z)$ of any point in the laminate space in terms of the thickness co-ordinate z. So

$$\begin{aligned}
u(x,\theta,z,t) &= u_0(x,\theta,t)+zu_1(x,\theta,t)\\
&\quad +z^2u_2(x,\theta,t)+z^3u_3(x,\theta,t),\\
v(x,\theta,z,t) &= (1+z/R)v_0(x,\theta,t)+zv_1(x,\theta,t)\\
&\quad +z^2v_2(x,\theta,t)+z^3v_3(x,\theta,t),\\
w(x,\theta,z,t) &= w_0(x,\theta,t)+zw_1(x,\theta,t)\\
&\quad +z^2w_2(x,\theta,t)
\end{aligned} \tag{1}$$

Where $u_0(x,\theta,z)$, $v_0(x,\theta,z)$ and $w_0(x,\theta,z)$ represent the displacements in axial, circumferential and radial directions respectively. $u_1(x,\theta,z)$ and $v_1(x,\theta,z)$ are the rotations of the normal to the element middle plane about the circumferential and axial directions. Also, $u_2(x,\theta,z)$, $v_2(x,\theta,z)$, $u_3(x,\theta,z)$, $v_3(x,\theta,z)$, $w_1(x,\theta,z)$ and $w_2(x,\theta,z)$ are the higher-order terms in the Taylor's series expansion and they represent higher-order transverse cross sectional deformation modes. In addition, strain tensor is expressed as:

$$\begin{aligned}
\varepsilon_{xx} &= \frac{\partial u}{\partial x}\\
\varepsilon_{\theta\theta} &= \left(\frac{1}{1+z/R}\right)\left(\frac{\partial v}{R\partial\theta}+\frac{w}{R}\right)\\
\varepsilon_{zz} &= \frac{\partial w}{\partial z}, \qquad \gamma_{xz} = \frac{\partial w}{\partial x}+\frac{\partial u}{\partial z},\\
\gamma_{x\theta} &= \left(\frac{\partial v}{\partial x}\right)+\left(\frac{1}{1+z/R}\right)\left(\frac{\partial u}{R\partial\theta}\right)\\
\gamma_{\theta z} &= \left(\frac{1}{1+z/R}\right)\left(\frac{\partial w}{R\partial\theta}-\frac{v}{R}\right)+\frac{\partial v}{\partial z}
\end{aligned} \tag{2}$$

Now, by substituting Eq. (1) into Eq. (2), one could obtain strain components:

$$\begin{aligned}
\varepsilon_{xx} &= \frac{\partial u_0}{\partial x}+z\frac{\partial u_1}{\partial x}+z^2\frac{\partial u_2}{\partial x}+z^3\frac{\partial u_3}{\partial x}\\
\varepsilon_{\theta\theta} &= \frac{1}{R(1+\frac{z}{R})}\begin{pmatrix}(1+\frac{z}{R})\frac{\partial v_0}{\partial\theta}+z\frac{\partial v_1}{\partial\theta}\\ +z^2\frac{\partial v_2}{\partial\theta}+z^3\frac{\partial v_3}{\partial\theta}\\ +w_0+zw_1+z^2w_2\end{pmatrix}\\
\varepsilon_{zz} &= w_1+2zw_2\\
\gamma_{x\theta} &= (1+\frac{z}{R})\frac{\partial v_0}{\partial x}+z\frac{\partial v_1}{\partial x}+z^2\frac{\partial v_2}{\partial x}+z^3\frac{\partial v_3}{\partial x}\\
&\quad +\frac{1}{R(1+\frac{z}{R})}\left(\frac{\partial u_0}{\partial\theta}+z\frac{\partial u_1}{\partial\theta}+z^2\frac{\partial u_2}{\partial\theta}+z^3\frac{\partial u_3}{\partial\theta}\right)\\
\gamma_{xz} &= \frac{\partial w_0}{\partial x}+z\frac{\partial w_1}{\partial x}+z^2\frac{\partial w_2}{\partial x}+u_1+2zu_2+3z^2u_3
\end{aligned} \tag{2}$$

$$\gamma_{\theta z}=\frac{1}{R(1+\frac{z}{R})}\begin{pmatrix}\frac{\partial w_0}{\partial\theta}+z\frac{\partial w_1}{\partial\theta}+z^2\frac{\partial w_2}{\partial\theta}\\ -(1+\frac{z}{R})v_0-zv_1-z^2v_2-z^3v_3\end{pmatrix}$$
$$+\left(\frac{v_0}{R}+v_1+2zv_2+3zv_3\right) \qquad (3)$$
$$\begin{Bmatrix}N_{zz}\\M_{zz}\\P_{zz}\\V_{zz}\end{Bmatrix}=\int_{-h/2}^{h/2}\sigma_{zz}\begin{Bmatrix}1\\z\\z^2\\z^3\end{Bmatrix}dz,\quad N^{**}_{x\theta}=\int_{-h/2}^{h/2}\sigma_{x\theta}\left(1+\frac{z}{R}\right)^2dz$$

n addition, the three-dimensional stress–strain relation can be expressed as follows:

$$\begin{bmatrix}\sigma_{xx}\\\sigma_{\theta\theta}\\\sigma_{zz}\\\sigma_{x\theta}\\\sigma_{xz}\\\sigma_{\theta z}\end{bmatrix}=\begin{bmatrix}\bar{Q}_{11}&\bar{Q}_{12}&\bar{Q}_{13}&0&0&0\\\bar{Q}_{12}&\bar{Q}_{22}&\bar{Q}_{23}&0&0&0\\\bar{Q}_{13}&\bar{Q}_{23}&\bar{Q}_{33}&0&0&0\\0&0&0&\bar{Q}_{44}&0&0\\0&0&0&0&\bar{Q}_{55}&0\\0&0&0&0&0&\bar{Q}_{66}\end{bmatrix}\begin{bmatrix}\varepsilon_{xx}-\alpha_1\Delta T\\\varepsilon_{\theta\theta}-\alpha_2\Delta T\\\varepsilon_{zz}-\alpha_3\Delta T\\\varepsilon_{x\theta}\\\varepsilon_{xz}\\\varepsilon_{\theta z}\end{bmatrix} \qquad (4)$$

In Eq. (4) α and ΔT are thermal expansion and temperature changes respectively. In addition, the stiffness coefficients are expressed as:

$$\bar{Q}_{11}=\frac{E_1(1-\nu_{23}\nu_{32})}{\nu^*},\ \bar{Q}_{12}=\frac{E_1(\nu_{21}+\nu_{31}\nu_{23})}{\nu^*},$$
$$\bar{Q}_{13}=\frac{E_1(\nu_{31}+\nu_{21}\nu_{32})}{\nu^*},\ \bar{Q}_{23}=\frac{E_2(\nu_{32}+\nu_{12}\nu_{31})}{\nu^*}$$
$$\bar{Q}_{22}=\frac{E_2(1-\nu_{13}\nu_{31})}{\nu^*} \qquad (5)$$
$$\bar{Q}_{44}=G_{12},\ \bar{Q}_{55}=G_{13},\ \bar{Q}_{66}=G_{23},$$
$$\nu^*=1-\nu_{12}\nu_{21}-\nu_{23}\nu_{32}-\nu_{13}\nu_{31}-2\nu_{21}\nu_{32}\nu_{13}$$

For the equations of the motion and boundary conditions, the principle of minimum potential energy states that (Tauchert, [22]):

$$\int_{t_1}^{t_2}(\delta T-\delta U+\delta W_1+\delta W_2)dt=0 \qquad (6)$$

Strain energy of spinning cylindrical thick shell conveying viscose fluid flow is expressed as follows:

$$\delta U=\frac{1}{2}\iiint_V(\sigma_{ij}\delta\varepsilon_{ij})\,dV=$$
$$\left[\begin{array}{l}\left(\begin{array}{l}N^*_{xx}\frac{\partial}{\partial x}\delta u_0+M^*_{xx}\frac{\partial}{\partial x}\delta u_1\\+P^*_{xx}\frac{\partial}{\partial x}\delta u_2+V^*_{xx}\frac{\partial}{\partial x}\delta u_3\end{array}\right)\\+\left(\frac{1}{R}\left(\begin{array}{l}N^*_{\theta\theta}\frac{\partial}{\partial\theta}\delta v_0+M_{\theta\theta}\frac{\partial}{\partial\theta}\delta v_1\\+P_{\theta\theta}\frac{\partial}{\partial\theta}\delta v_2+V_{\theta\theta}\frac{\partial}{\partial\theta}\delta v_3\\+N_{zz}\delta w_0+M_{zz}\delta w_1\\+P_{zz}\delta w_2\end{array}\right)\right)\\+\left(N^*_{zz}\delta w_1+2M^*_{zz}\delta w_2\right)\\+\left(\begin{array}{l}N^{**}_{x\theta}\frac{\partial}{\partial x}\delta v_0+M^*_{x\theta}\frac{\partial}{\partial x}\delta v_1\\+P^*_{x\theta}\frac{\partial}{\partial x}\delta v_2+V^*_{x\theta}\frac{\partial}{\partial x}\delta v_3\\+\frac{1}{R}\left(\begin{array}{l}N_{x\theta}\frac{\partial}{\partial\theta}\delta u_0+M_{x\theta}\frac{\partial}{\partial\theta}\delta u_1\\+P_{x\theta}\frac{\partial}{\partial\theta}\delta u_2+V_{x\theta}\frac{\partial}{\partial\theta}\delta u_3\end{array}\right)\end{array}\right)dV\\+\left(\begin{array}{l}Q^*_{xz}\frac{\partial}{\partial x}\delta w_0+S^*_{xz}\frac{\partial}{\partial x}\delta w_1\\+R^*_{xz}\frac{\partial}{\partial x}\delta w_2+Q^*_{xz}\delta u_1\\+2S^*_{xz}\delta u_2+3R^*_{xz}\delta u_3\end{array}\right)\\+\left(\frac{1}{R}\left(\begin{array}{l}Q_{\theta z}\frac{\partial}{\partial\theta}\delta w_0+S_{\theta z}\frac{\partial}{\partial\theta}\delta w_1\\+R_{\theta z}\frac{\partial}{\partial\theta}\delta w_2-Q^*_{\theta z}\delta v_0\\-S_{\theta z}\delta v_1-R_{\theta z}\delta v_2-O_{\theta z}\delta v_3\end{array}\right)\right)\\+\left(\begin{array}{l}Q^*_{\theta z}\frac{\delta v_0}{R}+Q^*_{\theta z}\delta v_1\\+2S^*_{\theta z}\delta v_2+3R^*_{\theta z}\delta v_3\end{array}\right)\end{array}\right] \qquad (7)$$

where, the components of the stress-resultant vector are defined as follows:

$$\begin{Bmatrix}N^*_{xx}\\M^*_{xx}\\P^*_{xx}\\V^*_{xx}\end{Bmatrix}=\int_{-h/2}^{h/2}\sigma_{xx}\left(1+\frac{z}{R}\right)\begin{Bmatrix}1\\z\\z^2\\z^3\end{Bmatrix}dz,$$
$$\begin{Bmatrix}N_{\theta\theta}\\M_{\theta\theta}\\P_{\theta\theta}\\V_{\theta\theta}\end{Bmatrix}=\int_{-h/2}^{h/2}\sigma_{\theta\theta}\begin{Bmatrix}1\\z\\z^2\\z^3\end{Bmatrix}dz, \qquad (8)$$
$$N^*_{\theta\theta}=\int_{-h/2}^{h/2}\sigma_{\theta\theta}\left(1+\frac{z}{R}\right)dz,$$
$$\begin{Bmatrix}N^*_{zz}\\M^*_{zz}\\P^*_{zz}\\V^*_{zz}\end{Bmatrix}=\int_{-h/2}^{h/2}\sigma_{zz}\left(1+\frac{z}{R}\right)\begin{Bmatrix}1\\z\\z^2\\z^3\end{Bmatrix}dz,$$

$$\begin{Bmatrix} N^*_{x\theta} \\ M^*_{x\theta} \\ P^*_{x\theta} \\ V^*_{x\theta} \end{Bmatrix} = \int_{-h/2}^{h/2} \sigma_{x\theta} \left(1+\frac{z}{R}\right) \begin{Bmatrix} 1 \\ z \\ z^2 \\ z^3 \end{Bmatrix} dz,$$

$$\begin{Bmatrix} N_{x\theta} \\ M_{x\theta} \\ P_{x\theta} \\ V_{x\theta} \end{Bmatrix} = \int_{-h/2}^{h/2} \sigma_{x\theta} \begin{Bmatrix} 1 \\ z \\ z^2 \\ z^3 \end{Bmatrix} dz,$$

$$\begin{Bmatrix} Q^*_{xz} \\ S^*_{xz} \\ R^*_{xz} \\ O^*_{xz} \end{Bmatrix} = \int_{-h/2}^{h/2} \sigma_{xz} \left(1+\frac{z}{R}\right) \begin{Bmatrix} 1 \\ z \\ z^2 \\ z^3 \end{Bmatrix} dz, \quad (8)$$

$$\begin{Bmatrix} Q_{\theta z} \\ S_{\theta z} \\ R_{\theta z} \\ O_{\theta z} \end{Bmatrix} = \int_{-h/2}^{h/2} \sigma_{\theta z} \begin{Bmatrix} 1 \\ z \\ z^2 \\ z^3 \end{Bmatrix} dz,$$

$$\begin{Bmatrix} Q^*_{\theta z} \\ S^*_{\theta z} \\ R^*_{\theta z} \\ O^*_{\theta z} \end{Bmatrix} = \int_{-h/2}^{h/2} \sigma_{\theta z} \left(1+\frac{z}{R}\right) \begin{Bmatrix} 1 \\ z \\ z^2 \\ z^3 \end{Bmatrix} dz,$$

The velocity vector of any generic point on a rotating cylindrical shell is expressed as:

$$V = \frac{\partial u}{\partial t} i + \left(\frac{\partial v}{\partial t} + \Omega w\right) j + \left(\frac{\partial w}{\partial t} - \Omega v\right) k \quad (9)$$

The first three terms are results from linear velocities in axial, circumferential and lateral directions, respectively. The fourth and fifth terms are coriolis and centrifugal effects. Over-doted terms represent temporal derivatives. i, j, and k are unit vectors in the x, θ and z directions, respectively. Furthermore, the kinetic energy of a cylindrical shell can be expressed as:

$$\delta T = \int_Z \iint_A \rho \begin{bmatrix} \left(\frac{\partial u}{\partial t}\right)\left(\frac{\partial \delta u}{\partial t}\right) + \\ \left(\frac{\partial v}{\partial t} + \Omega w\right)\left(\frac{\partial \delta v}{\partial t} + \Omega \delta w\right) \\ + \left(\frac{\partial w}{\partial t} - \Omega v\right)\left(\frac{\partial \delta w}{\partial t} - \Omega \delta v\right) \end{bmatrix} \times \left(R dx\, d\theta\, dz\right) \quad (10)$$

Consider the flow of fluid in a cylindrical shell in which the flow is assumed to be axially symmetric, Newtonian, and laminar [23]. By the well-known Navier–Stokes equation, the basic momentum governing equation of the flow is simplified as:

$$\rho_b \frac{dV_R}{dt} = -\frac{\partial P}{\partial R} + \frac{1}{R}\frac{\partial \tau_{R\theta}}{\partial \theta} - \frac{\tau_{\theta\theta}}{R} + \frac{\partial \tau_{Rx}}{\partial x} \quad (11)$$

In Eq (11), P and ρ_b are flow fluid pressure and mass density of the fluid respectively. The fluid force act on the cylindrical shell can be calculated from Eq. (11). Since the acceleration and the velocity of the cylindrical shell and fluid at the contact point between them are equal [23], there are the relations below:

$$v_R = \frac{dw_0}{dt}, \quad \frac{d}{dt} = \frac{\partial}{\partial t} + v_x \frac{\partial}{\partial x} \quad (12)$$

where v_x is the mean flow velocity. In Eq. (12), shear stress (τ) depends on the viscosity (μ) which can be obtained as below:

$$\tau_{R\theta} = \frac{\mu}{R}\frac{\partial V_R}{\partial \theta}, \quad \tau_{\theta\theta} = 2\mu\frac{V_R}{R}, \quad \tau_{Rx} = \mu\frac{\partial V_R}{\partial x} \quad (13)$$

Finally, using Eqs. (12) and (13), and combining them with Eq. (11), the pressure of fluid ($\frac{\partial P}{\partial R}$) will be obtained. The fluid flow work may be written as:

$$\delta W_1 = \int_0^{2\pi}\int_0^L \frac{\partial P}{\partial R} R\, dx\, d\theta \quad (14)$$

The axial fluid velocity in the above relation can be written as:

$$v_x = v_{ave,slip} = VCF \times v_{ave,noslip} \quad (15)$$

where, the modified dimensionless coefficient VCF may be defined as:

$$VCF = (1+aK_n) \times \left[1 + 4\left(\left(\frac{2-\sigma_v}{\sigma_v}\right)\left(\frac{k_n}{1+k_n}\right)\right)\right] \quad (16)$$

where, the slip of flow from inner cylindrical shell through the number of Knudsen (k_n) is considered. Practically, it is supposed to be σ_v =0.7; in addition, other parameters are:

$$a = a_0 \frac{2}{\pi}(\tan^{-1}(a_1 k_n^B)),\ a_0 = \frac{64}{3\pi}\left(1-\frac{4}{b}\right)^{-1}, \quad \mu = \mu_0(1+ak_n)^{-1} \quad (17)$$

In Eq. (17), μ and μ_0 are fluid viscosity and bulk viscosity respectively.For a typical isotropic cylindrical shell which is in high temperature environment, it is assumed that the temperature can be distributed across its thickness. Hence, the first variation of the work done corresponding to the temperature change can be obtained as (SafarPour et al., [24]):

$$\delta W_2 = \iint_A \left[N_1^T \frac{\partial w_0}{\partial x}\frac{\partial \delta w_0}{\partial x} + N_2^T \frac{\partial v_0}{\partial x}\frac{\partial \delta v_0}{\partial x} \right] R\, dx\, d\theta \qquad (18)$$

where N_1^T and N_2^T are the thermal resultants. Note that the two thermal resultants can be expressed as:

$$N_1^T = \int_{-h/2}^{h/2} (\bar{Q}_{11} + \bar{Q}_{12} + \bar{Q}_{13})\, \alpha (T - T_0) dz,$$
$$N_2^T = \int_{-h/2}^{h/2} (\bar{Q}_{21} + \bar{Q}_{22} + \bar{Q}_{23})\, \alpha (T - T_0) dz. \qquad (19)$$

Thermal expansion coefficients are given by Kadoli and Ganesan (Kadoli and Ganesan, [25]) as:

$$\alpha = \begin{bmatrix} \alpha_{xxe} & \alpha_{\theta\theta e} & \alpha_{zze} & 0 & 0 & 0 \end{bmatrix}^T \qquad (20)$$

It is assumed that the temperature varies linearly along the thickness from T_m at the outer surface to T_c at the inner surface.

A- Linear temperature rise (LT)

It is assumed that the temperature varies linearly along the thickness from T_m at the outer surface to T_c at the inner surface. The temperature variations can be written as follows (Shahsiah and Eslami, [14]):

$$T = T_c - \Delta T \left(\frac{1}{2} + \frac{\hat{z}_c}{h}\right) \qquad (21a)$$

in which ΔT is defined as $\Delta T = T_c - T_m$.

Nonlinear temperature rise (NLT)

In this case, nonlinear temperature rise across the thickness is assumed. The temperature variations can be written as follows (Shafiei et al., [26]).

$$T = T_c - \Delta T \left(\frac{1}{2} + \frac{\hat{z}_c}{h}\right)^{\alpha_p} \qquad (21b)$$

where α_p denotes the non-negative power index of temperature variation function and $\Delta T = T_c - T_m$. For example, considering $\alpha_p \geq 2$ the temperature variation along the thickness becomes nonlinear. The work done by Winkler foundation acting on the free supported of the cylindrical shell can be expressed as (Zeighampour and Beni, [27]):

$$\delta W_b = \{K_w w\}\, \delta w\, R\, dV \qquad (22)$$

in which K_W is the Winkler coefficient. The Winkler foundation, will be added to the structure in $x=L/2$. It is worth mentioning that, the mass system in the boundary condition will be added to boundary elements. Substituting Eqs. (7), (10), (14) and (18) into Eq. (6) and integrating by part, the equations of motion and boundary conditions of the spinning cylindrical thick shell carrying spring- mass systems and conveying viscos fluid flow can be obtained as follows using the RHOST:

$$\delta u_0 : \frac{\partial N_{xx}^*}{\partial x} + \frac{1}{R}\frac{\partial N_{x\theta}}{\partial \theta} = I_0 \frac{\partial^2 u_0}{\partial t^2} + I_1 \frac{\partial^2 u_1}{\partial t^2} + I_2 \frac{\partial^2 u_2}{\partial t^2} + I_3 \frac{\partial^2 u_3}{\partial t^2}$$

$$\delta v_0 : \frac{1}{R}\frac{\partial N_{\theta\theta}^*}{\partial \theta} + \frac{\partial N_{x\theta}^{**}}{\partial x} - N_2^T \frac{\partial^2 v_0}{\partial x^2} = I_0^* \frac{\partial^2 v_0}{\partial t^2} + I_1 \frac{\partial^2 v_1}{\partial t^2} + I_2 \frac{\partial^2 v_2}{\partial t^2} + I_3 \frac{\partial^2 v_3}{\partial t^2} + 2\Omega \left[I_0 \frac{\partial^2 w_0}{\partial t^2} + I_1 \frac{\partial^2 w_1}{\partial t^2} + I_2 \frac{\partial^2 w_2}{\partial t^2} \right] - \Omega^2 \left[I_0^* v_0 + I_1 v_1 + I_2 v_2 + I_3 v_3 \right]$$

$$\delta w_0 : \frac{\partial Q_{xz}^*}{\partial x} + \frac{1}{R}\frac{\partial Q_{\theta z}}{\partial \theta} - \frac{1}{R} N_{\theta\theta} - \varsigma_1 v_x^2 \frac{\partial^2 w}{\partial x^2} - \varsigma_2 v_x \frac{\partial w}{\partial x} + \varsigma_3 v_x \frac{\partial^3 w}{\partial x^3} - N_1^T \frac{\partial^2 w_0}{\partial x^2} = I_0 \frac{\partial^2 w_0}{\partial t^2} + I_1 \frac{\partial^2 w_1}{\partial t^2} + I_2 \frac{\partial^2 w_2}{\partial t^2} + \varsigma_4 \frac{\partial^2 w}{\partial t^2} - \varsigma_5 v_x \frac{\partial^2 w}{\partial x \partial t} - \varsigma_6 \frac{\partial w}{\partial t} + \varsigma_7 \frac{\partial^3 w}{\partial t \partial x^2} - 2\Omega \left[\begin{matrix} I_0 \frac{\partial^2 v_0}{\partial t^2} + I_1 \frac{\partial^2 v_1}{\partial t^2} \\ + I_2 \frac{\partial^2 v_2}{\partial t^2} + I_3 \frac{\partial^2 v_3}{\partial t^2} \end{matrix} \right] - \Omega^2 \left[I_0 w_0 + I_1 w_1 + I_2 w_2 \right] \qquad (23)$$

$$\delta u_1 : \frac{\partial M_{xx}^*}{\partial x} + \frac{1}{R}\frac{\partial M_{x\theta}}{\partial \theta} - Q_{xz}^* = I_1 \frac{\partial^2 u_0}{\partial t^2} + I_2 \frac{\partial^2 u_1}{\partial t^2} + I_3 \frac{\partial^2 u_2}{\partial t^2} + I_4 \frac{\partial^2 u_3}{\partial t^2}$$

$$\delta v_1 : \frac{1}{R}\frac{\partial M_{\theta\theta}}{\partial \theta} + \frac{\partial M_{x\theta}^*}{\partial x} + \frac{1}{R} S_{\theta z} - Q_{\theta z}^* = I_1^* \frac{\partial^2 v_0}{\partial t^2} + I_2 \frac{\partial^2 v_1}{\partial t^2} + I_3 \frac{\partial^2 v_2}{\partial t^2} + I_4 \frac{\partial^2 v_3}{\partial t^2} + 2\Omega \left[I_1 \frac{\partial^2 w_0}{\partial t^2} + I_2 \frac{\partial^2 w_1}{\partial t^2} + I_3 \frac{\partial^2 w_2}{\partial t^2} \right] - \Omega^2 \left[I_1^* v_0 + I_2 v_1 + I_3 v_2 + I_4 v_3 \right]$$

$$\delta w_1 : \frac{\partial S_{xz}^*}{\partial x} + \frac{1}{R}\frac{\partial S_{\theta z}}{\partial \theta} - \frac{1}{R} M_{\theta\theta} - N_{zz}^* = I_1 \frac{\partial^2 w_0}{\partial t^2} + I_2 \frac{\partial^2 w_1}{\partial t^2} + I_3 \frac{\partial^2 w_2}{\partial t^2}$$

$$-2\Omega\left[I_1\frac{\partial^2 v_0}{\partial t^2}+I_2\frac{\partial^2 v_1}{\partial t^2}+I_3\frac{\partial^2 v_2}{\partial t^2}+I_4\frac{\partial^2 v_3}{\partial t^2}\right]$$
$$-\Omega^2\left[I_1 w_0+I_2 w_1+I_3 w_2\right]$$

$$\delta u_2:\frac{\partial P^*_{xx}}{\partial x}+\frac{1}{R}\frac{\partial P_{x\theta}}{\partial \theta}-2S^*_{xz}=$$
$$I_2\frac{\partial^2 u_0}{\partial t^2}+I_3\frac{\partial^2 u_1}{\partial t^2}+I_4\frac{\partial^2 u_2}{\partial t^2}+I_5\frac{\partial^2 u_3}{\partial t^2}$$

$$\delta v_2:\frac{1}{R}\frac{\partial P_{\theta\theta}}{\partial \theta}+\frac{\partial P^*_{x\theta}}{\partial x}+\frac{1}{R}R_{\theta z}-2S^*_{\theta z}=$$
$$I^*_2\frac{\partial^2 v_0}{\partial t^2}+I_3\frac{\partial^2 v_1}{\partial t^2}+I_4\frac{\partial^2 v_2}{\partial t^2}+I_5\frac{\partial^2 v_3}{\partial t^2}$$
$$+2\Omega\left[I_2\frac{\partial^2 w_0}{\partial t^2}+I_3\frac{\partial^2 w_1}{\partial t^2}+I_4\frac{\partial^2 w_2}{\partial t^2}\right]$$
$$-\Omega^2\left[I^*_2 v_0+I_3 v_1+I_3 v_4+I_4 v_5\right]$$

$$\delta w_2:\frac{\partial R^*_{xz}}{\partial x}+\frac{1}{R}\frac{\partial R_{\theta z}}{\partial \theta}-\frac{1}{R}P_{\theta\theta}-2M^*_{zz}=$$
$$I_2\frac{\partial^2 w_0}{\partial t^2}+I_3\frac{\partial^2 w_1}{\partial t^2}+I_4\frac{\partial^2 w_2}{\partial t^2}$$
$$-2\Omega\left[\begin{array}{l}I_2\frac{\partial^2 v_0}{\partial t^2}+I_3\frac{\partial^2 v_1}{\partial t^2}\\+I_4\frac{\partial^2 v_2}{\partial t^2}+I_5\frac{\partial^2 v_3}{\partial t^2}\end{array}\right]$$
$$-\Omega^2\left[I_2 w_0+I_3 w_1+I_4 w_2\right]$$

$$\delta u_3:\frac{\partial V^*_{xx}}{\partial x}+\frac{1}{R}\frac{\partial V_{x\theta}}{\partial \theta}-3R^*_{xz}=I_3\frac{\partial^2 u_0}{\partial t^2}$$
$$+I_4\frac{\partial^2 u_1}{\partial t^2}+I_5\frac{\partial^2 u_2}{\partial t^2}+I_6\frac{\partial^2 u_3}{\partial t^2}$$

$$\delta v_3:\frac{1}{R}\frac{\partial V_{\theta\theta}}{\partial \theta}+\frac{\partial V^*_{x\theta}}{\partial x}+\frac{1}{R}O_{\theta z}-3R^*_{\theta z}=I^*_3\frac{\partial^2 v_0}{\partial t^2}$$
$$+I_4\frac{\partial^2 v_1}{\partial t^2}+I_5\frac{\partial^2 v_2}{\partial t^2}+I_6\frac{\partial^2 v_3}{\partial t^2}$$
$$+2\Omega\left[I_3\frac{\partial^2 w_0}{\partial t^2}+I_4\frac{\partial^2 w_1}{\partial t^2}+I_5\frac{\partial^2 w_2}{\partial t^2}\right]$$
$$-\Omega^2\left[I^*_3 v_0+I_4 v_1+I_5 v_2+I_6 v_3\right]$$

The boundary conditions are as below:

$$\begin{array}{lll}
\delta u_0=0 & or & N^*_{xx}d\theta+\frac{N_{x\theta}}{R}dx=0\\
\delta v_0=0 & or & N^{**}_{x\theta}d\theta+\frac{N^*_{\theta\theta}}{R}dx=0\\
\delta w_0=0 & or & Q^*_{xz}d\theta+\frac{Q_{\theta z}}{R}dx=0\\
\delta u_1=0 & or & M^*_{xx}d\theta+\frac{M_{x\theta}}{R}dx=0\\
\delta v_1=0 & or & M^*_{x\theta}d\theta+\frac{M_{\theta\theta}}{R}dx=0\\
\delta w_1=0 & or & S^*_{xz}d\theta+\frac{S_{\theta z}}{R}dx=0\\
\delta u_2=0 & or & P^*_{xx}d\theta+\frac{P_{x\theta}}{R}dx=0\\
\delta v_2=0 & or & P^*_{x\theta}d\theta+\frac{P_{\theta\theta}}{R}dx=0\\
\delta w_2=0 & or & R^*_{xz}d\theta+\frac{R_{\theta z}}{R}dx=0\\
\delta u_3=0 & or & V^*_{xx}d\theta+\frac{V_{x\theta}}{R}dx=0\\
\delta v_3=0 & or & V^*_{x\theta}d\theta+\frac{V_{\theta\theta}}{R}dx=0
\end{array}\qquad (24)$$

Appendix describes the parameters used in Eqs (23) and (24).

Solution procedure

In this section, short reviews of semi-numerical solutions of the governing equations are presented. As respects, the semi-numerical solution is obtainedutilizing generalized differential quadrature method (GDQ) is presented for the structure prescribed by the varus boundary conditions.

Generalized differential quadrature method (GDQ) has been exhaustively used to solve the governing equations of motion in these structures (Ghadiri et al., [28]; Barooti et al., [29]; SafarPour and Ghadiri, [30]). Literature review reveals the deficiency of investigations in analyzing thick cylindrical shells and centrifugal force. In this work, GDQ method is used to calculate the spatial derivatives of field variables in equilibrium equations. In implementation of GDQ, grid points define the locations of calculated derivatives and field variables. Therefore, the "r – th" order derivative of a function "f(x)" can be defined as linear sum of the function values which is (Shu, [31]) :

$$\left.\frac{\partial^r f(x)}{\partial x^r}\right|_{x=x_P} = \sum_{j=1}^{n} C_{ij}^{(r)} f(x_i) \tag{25}$$

Where, n is the number of grid points along x direction. As well as, C_{ij} is obtained as follows:

$$C_{ij}^{(1)} = \begin{cases} \dfrac{M(r_i)}{(r_i - r_j) M(r_j)} & i \neq j \\ -\sum_{j=1, i\neq j}^{n} C_{ij}^{(1)} & i = j \end{cases} \tag{26}$$

and M is determined as:

$$M(x_i) = \prod_{j=1, j\neq i}^{n} (x_i - x_j) \tag{27}$$

Superscript "r" is the order of derivative. Also, C(r) is the weighing coefficient along x direction which could be written as:

$$C_{ij}^{(r)} = \begin{cases} r\left[C_{ij}^{(r-1)} C_{ij}^{(1)} - \dfrac{C_{ij}^{(r-1)}}{(r_i - r_j)}\right] & \begin{cases} i \neq j \\ and \\ 2 \leq r \leq n-1 \end{cases} \\ -\sum_{j=1, i\neq j}^{n} C_{ij}^{(r)} & \begin{cases} i = j \\ and \\ 1 \leq r \leq n-1 \end{cases} \end{cases} \tag{28}$$

Owing to the geometrical periodicity of the cylindrical shell, displacement vector for free vibration analysis can be described as follow:

$$\begin{Bmatrix} u_i(x,\theta,t) \\ v_i(x,\theta,t) \\ w_i(x,\theta,t) \end{Bmatrix} = \sum_{n=1}^{\infty} \begin{Bmatrix} \overline{U}_i(x)\cos(n\theta) e^{i\omega t} \\ \overline{V}_i(x)\sin(n\theta) e^{i\omega t} \\ \overline{W}_i(x)\cos(n\theta) e^{i\omega t} \end{Bmatrix} \tag{29}$$

A proper method to discretize the domain is applying Chebyshev polynomials as it is explained in (Civalek, [32]). Now the following equation is obtained by substituting Eq. (29) into equations Eq. (17):

$$\left([M]\{\omega^2\} + [C]\{\omega\} + [K]\right)\begin{pmatrix} d_b \\ d_d \end{pmatrix} = 0 \tag{30}$$

Stiffness matrix [K], damping matrix [C] and mass matrix [M] are obtained by applying GDQ into the equations of motion and the boundary conditions. Moreover, d and b indexes denote the domain and boundary respectively and d also is the shape of the mode. For solving Eq. (30) and reducing it to the standard form of eigenvalue problem, a convenient way is to rewrite Eq. (30) as the following the first order variable:

$$\{\dot{z}\} = \{A\}\{Z\} \tag{31}$$

In which, state vector Z and state matrix [A] are defined as:

$$Z = \begin{Bmatrix} d_d \\ \dot{d}_d \end{Bmatrix} \tag{32}$$

and

$$[A] = \begin{bmatrix} [0] & [I] \\ -[M^{-1}K] & -[M^{-1}C] \end{bmatrix}$$

In Eq. (32), [0] and [I] are the zero and unit (identity) matrices, respectively. Eventually the natural frequency and its mode shape are obtained. It is worth mentioning that, the spring-mass systems will be added to boundary and middle elements.

Results and discussion

Here, the results of influence of rotation, velocity of fluid flow and thermal loading on the vibration behavior of the spinning cylindrical thick shell carrying spring- mass systems and conveying viscos fluid flow are in vestigate for the clamp-Free boundary condition. Sufficient numbers of grid points must be found to obtain accurate results for GDQ method. As it can be seen in Table 1, for getting the convergent results, 35 grid points are appropriate. However, results are presented by two sections, the first one presents a validation of the proposed model with previous literatures. The second section presents, the influence of various parameters on vibrational behavior of the spinning cylindrical thick shell carrying spring- mass systems and conveying viscos fluid flow.

Table1. The effect of the number of grid points on evaluating convergence of the dimensionless natural frequency ($\bar{\omega} = \omega R\sqrt{I_0 / A_{11}}$) of the cylindrical thick shell with respect to the frequency number and

$\Phi = 500m/s, M = 0, L/R = 0.3, R/h = 0.3, \Delta T = 100$

	Unit m/s	N=20	N=25	N=35	N=40
k_w=0	V=0	0.1679	0.1679	0.1679	0.16792
	V=500	0.1652	0.1652	0.1653	0.16531
	V=1000	0.1561	0.1562	0.1562	0.15625
k_w= $1e^{15}$	V=0	0.2358	0.2358	0.2358	0.23588
	V=500	0.2280	0.2280	0.2280	0.22804
	V=1000	0.2017	0.2017	0.2017	0.20177
k_w= $1e^{18}$	V=0	0.2558	0.2558	0.2558	0.25588
	V=500	0.2380	0.2380	0.2380	0.23804
	V=1000	0.2217	0.2217	0.2217	0.22177

model validation

For results verification of this work with other articles, Table 2 and Table 3 give a comparison of results for dimensionless natural frequency, of the simply supported cylindrical thick shell between the presented results with those obtained by other articles, for different geometrical parameters. It is worth mentioning that, in these articles the influences of rotation, velocity of fluid, and spring-mass systems are ignored.

Table2. Comparison of natural frequency parameters $\bar{\omega} = \omega h / \pi\sqrt{\rho / G}$ for simply supported isotropic cylindrical thick shell (m=n=1, h/R=0.06, G=E/2(1+ν))

L/R	Ref (Mirsky and Herrman n, [33])	Ref (Reddy, [34])	Ref (Khalili et al., [6])	Ref (Armenà kas et al., [35])	Present study
0.25	0.0861	0.0863	0.0863	0.0863	0.0863
0.5	0.0369	0.0369	0.0368	0.0369	0.0370
1	0.0278	0.0278	0.0278	0.0278	0.0276
2	0.0185	0.0185	0.0185	0.0185	0.0185

Table 3 shows the obtained results for dimensionless natural frequency of simply supported cylindrical thick shell for various thickness to length ratio. They are in good agreement with those given by Refs (Loy and Lam, [36]; Armenàkas et al., [35]; Khalili et al., [6]).

Table3. Comparison of natural frequency parameters $\bar{\omega} = \omega h / \pi\sqrt{\rho / G}$ for simply supported isotropic cylindrical thick shell (m=n=1, h/R=2)

h/L	Ref (Loy and Lam, [36])	Ref (Armenàkas et al., [35])	Ref (Khalili et al., [6])	Present study
0.01	0.000258	0.000253	0.00290	0.00273
0.1	0.02434	0.02423	0.03669	0.03456
0.2	0.08709	0.08703	0.10004	0.10400
0.4	0.26659	0.26658	0.27694	0.27365
0.6	0.468256	0.46827	0.47580	0.46950
0.8	0.67316	0.67316	0.67821	0.67520
1	0.87665	0.87660	0.87977	0.87860

In Table4, fundamental frequency of simply supported cylindrical thick shell that presented in this paper against those calculated by Refs (Loy and Lam, [36]; Armenàkas et al., [35]; Khalili et al., [6]) for a different range of thickness to radius ratio are compared, present results are in good agreement with the results.

Table4. Comparison of natural frequency parameters $\bar{\omega} = \omega h / \pi\sqrt{\rho / G}$ for simply supported isotropic cylindrical thick shell (m=n=1, h/L=0.2)

h/R	Ref (Loy and Lam, [36])	Ref (Armenàkas et al., [35])	Ref (Khalili et al., [6])	Present study
0.01	0.05774	0.05774	0.05774	0.05774
0.1	0.07618	0.07618	0.07606	0.07606
0.2	0.10704	0.10704	0.10680	0.10680
2	0.08704	0.08703	0.10003	0.08810

For another verification for this work, according to table5, it is revealed that the proposed modeling can provide good agreement with Loy et al (Loy et al., [37]) where the influences of rotation, velocity of fluid, and spring-mass systems are ignored.

Table 5. Comparison of dimensionless natural frequency of cylindrical shells for different values of circumferential wave number (n) with*L/R=20, R/h=100*.

N	Loy et al. [37]	Present	Error (%)
1	0.016101	0.0158099	0.18
2	0.009382	0.0092548	1.36
3	0.022105	0.0217143	0.17
4	0.042095	0.0413625	0.17

Parametric results

The mechanical properties of a cylindrical thick shell are given in Table 6. Now, in this section the effects of the, velocity of viscous fluid flow, angular velocity, temperature changes and spring-mass systems on the critical speed, critical velocity, critical temperature and natural frequency of the structure are investigated.

Table 6. The material properties of aluminum

$E=72.4\ GPa$, $\vartheta=0.3$, $\rho=2770\ kg/m^3$
$\alpha=22.5\times10^{-6}K^{-1}$

The effects of different temperature changes, coefficient of the spring and angular velocity on natural frequency and critical velocity of viscous fluid flow

Figs 3-4 demonstrate natural frequency versus the velocity of fluid flow for a cylindrical thick shell on different nonlinear temperature changes, angular velocity and the coefficient of the spring in $x=L/2$, respectively. The figure 3 shows that an increase in nonlinear temperature changes decrease the critical velocity of fluid flow and causes a decrease in stability of the structure. This is because of the fact that an increase in nonlinear temperature changes leads to a decrease in the stiffness of structure, and causes natural frequency and stability to decrease.

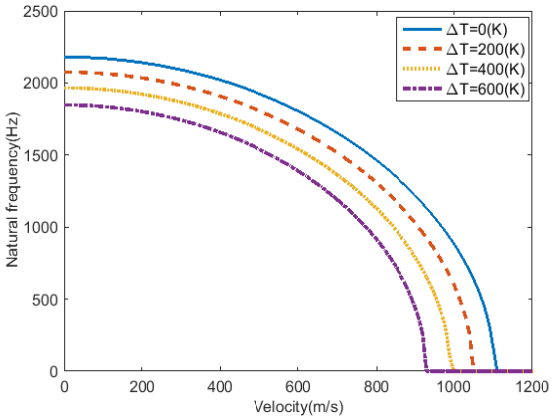

Figure 3. The variation of fundamentalfrequency (Hz) versus the velocity of fluid flow of a rotating cylindrical thick shell conveying viscous flow with differentnonlinear temperature changes with L/R=0.1, R/h=0.3, $K_W = 10^8 (N/m)$ and $\Phi = 100(m/s)$

In addition, by increasing the velocity of fluid flow, the natural frequency and dynamic stability of structure decrease. It can be seen from the figure 4 that in fundamental frequency, the increase in angular speed leads to the decrease in the frequency. This is because, by increasing the angular velocity, the dynamic stability of structure decrease. As it can be seen from figure4, an increase in coefficient of the spring leads to an increase in the fundamental frequency and critical velocity of fluid flow. This is because increasing the coefficient of the spring is eventuated to increase in stiffness and natural frequency of the structure.

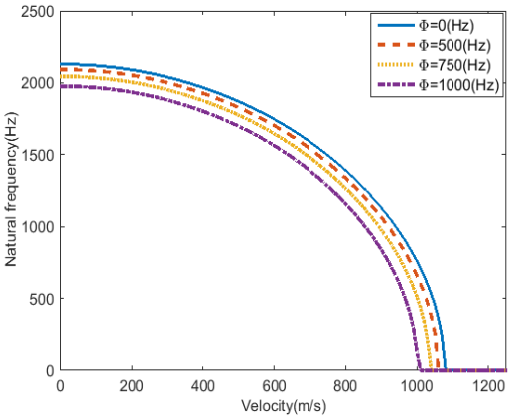

Figure 4. The variation of fundamental frequency (Hz) versus the velocity of fluid flow of a rotating cylindrical thick shell conveying viscous flow with different angular velocity with L/R=0.1, R/h=0.3, $K_W = 10^8 (N/m)$ and $\Delta T(Nonlinear) = 100(K)$

The Effects of Different Temperature Changes, Velocity of Viscous Fluid Flow, Coefficient of The Spring and Thermal Distributions on Natural Frequency and Critical Velocity

Figs 5-8show natural frequency versus angular velocity for different nonlinear temperature changes, viscous fluid flow, coefficient of the spring and thermal distributions, respectively. It can be seen from the figure 5 that as the nonlinear temperature changes increases, the critical speed of rotation decreases, this leads to a decrease in the instability of structure. This effect is more significant in higher angular velocities.

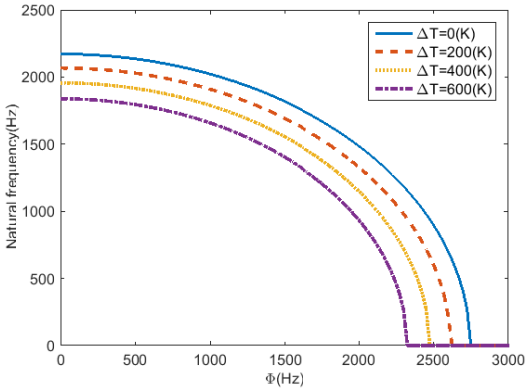

Figure 5.The variation of fundamental frequency (Hz) versus the angular velocity of a rotating cylindrical thick shell conveying viscous flow with different nonlinear temperature changes with L/R=0.1, R/h=0.3, $K_w = 10^8 (N/m)$ and $V = 100m/s$.

It can be seen from the figure 6 that in fundamental frequency, the increase in velocity of viscous fluid flow leads to the decrease in the frequency. This is because, by increasing the viscous fluid flow, the dynamic stability of the structure decrease.

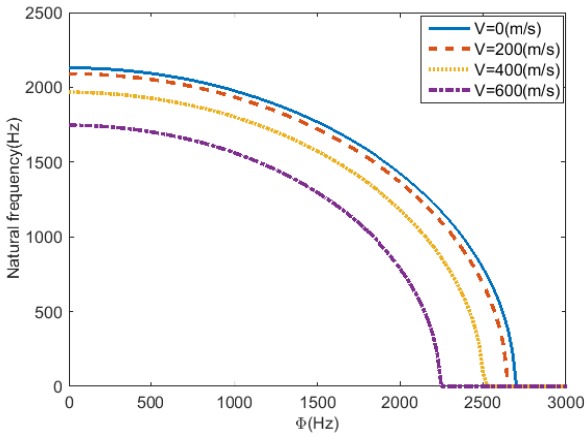

Figure 6. The variation of fundamental frequency (Hz) versus the angular velocity of a rotating cylindrical thick shell conveying viscous flow with different velocity of fluid flow with L/R=0.1, R/h=0.3, $K_w = 10^8 (N/m)$ and $\Delta T(Nonlinear) = 100(K)$.

As it can be seen from figure 7, an increase in coefficient of the spring leads to an increase in the critical speed of rotation.

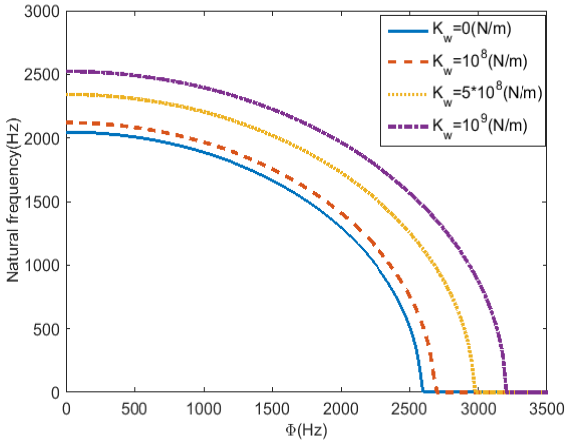

Figure 7. The variation of fundamental frequency (Hz) versus the angular velocity of a rotating cylindrical thick shell conveying viscous flow with different coefficient of the spring with L/R=0.1, R/h=0.3, $V = 100(m/s)$ and $\Delta T(Nonlinear) = 100(K)$.

As it can be observed from figure 8, whenever $\Phi < 1200(Hz)$, the uniform thermal distribution has the lower fundamental frequency in comparison with other thermal distributions. Also, in the higher angular velocity ($\Phi > 1200(Hz)$) the nonlinear thermal distribution has the highest fundamental frequency in comparison with other thermal distribution. Also, the figure shows that, the nonlinear thermal distribution has the higher stability area in comparison with other thermal distributions. So, the angular velocity parameter has a great influence on the natural frequency of the cantilever cylindrical thick shell.

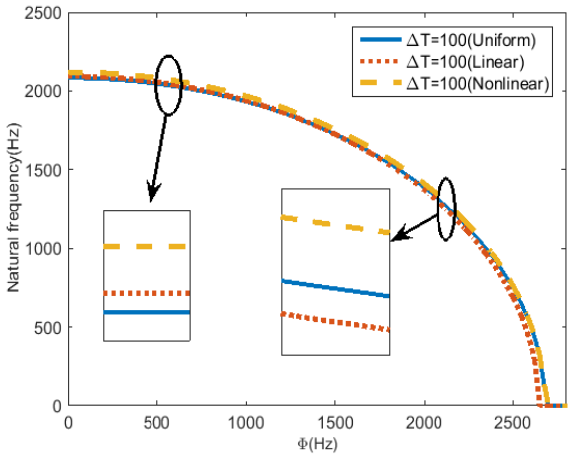

Figure 8. The variation of fundamental frequency (Hz) versus the angular velocity of a rotating cylindrical thick shell conveying viscous flow with various thermal distributions with L/R=0.1, R/h=0.3, $V = 100(m/s)$ and $K_W = 10^8 (N/m)$.

The Effect of Different Lumped Mass And Coefficient of The Spring on Natural Frequency and Critical Temperature Changes

Figures 9and 10 present the influence of lumped mass and coefficient of the spring on natural frequency and critical temperature changes, respectively. As it can be observed from figures 9 and 10,whenever $\Delta T(Nonlinear) < 5800(K)$, by increasing the lumped mass or coefficient of the spring, the natural frequency tends to decrease. Also, in the higher nonlinear temperature changes ($\Delta T > 5800(K)$), by increasing the lumped mass at the free end, the natural frequency tends to increase. Also, it can also be concluded from Figures 9 and 10, in the higher nonlinear temperature changes, by increasing the lumped mass or coefficient of the spring, the critical nonlinear temperature changes increase. So, the nonlinear temperature change parameter has a great influence on the frequency of the cantilever

cylindrical thick shell carrying spring-mass systems.

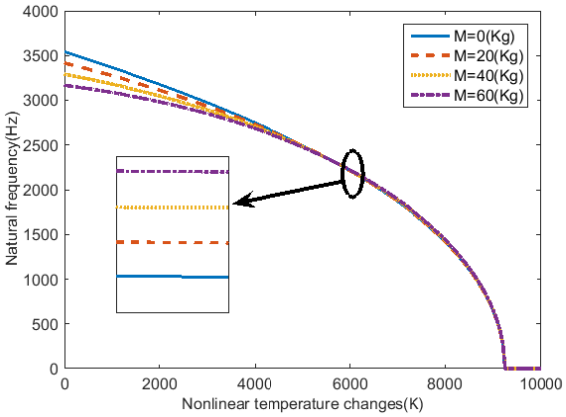

Figure9. The variation of fundamental frequency (Hz) versus the nonlinear temperature changes of a rotating cylindrical thick shell conveying viscous flow with different coefficient of the lumped mass at the free end with L/R=0.3, R/h=0.3, $\Phi = V = 0(m/s)$ and $K_W = 0(N/m)$.

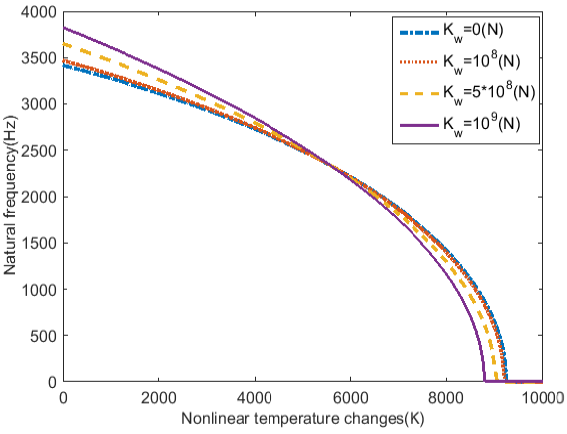

Figure 10.The variation of fundamental frequency (Hz) versus the nonlinear temperature changes of a rotating cylindrical thick shell conveying viscous flow with different coefficient of the spring with L/R=0.3, R/h=0.3, $V = \Phi = 0(m/s)$ and $M = 20(Kg)$.

The Effect of Different Coefficient of The Spring On Natural Frequency for Different Values of Lumped Mass At The Free end

Figure 11 illustrates natural frequency versus lumped mass at the free end for different coefficient of spring. It can be seen, from fig. 12, that an increase in the lumped mass at the free end causes a decrease in the natural frequency of the structure. This is because of the fact that an increase in lumped mass coefficient leads to a decrease in the stiffness of structure, and causes natural frequency and stability to decrease. Also, in all values of the lumped mass at the free end, by increasing the Winkler coefficient, the natural frequency tends to increase.

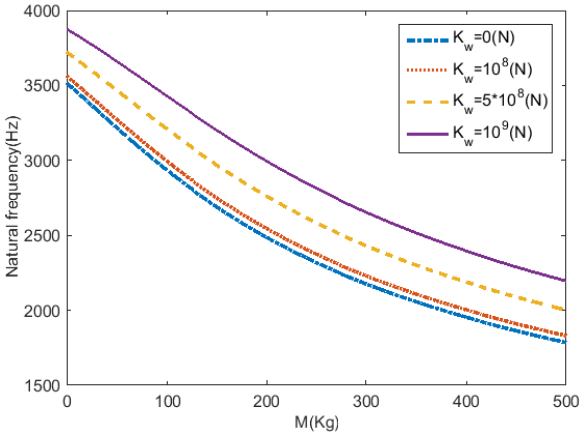

Figure 11. The variation of fundamental frequency (Hz) versus the coefficient of the lumped mass at the free end of a rotating cylindrical thick shell conveying viscous flow with different coefficient of the spring with L/R=0.3, R/h=0.3, $V = \Phi = 0(m/s)$ and $\Delta T(Linear) = 100(K)$.

Conclusion

This article presents the vibration analysis of a spinning cylindrical thick shell carrying spring- mass systems and conveying viscos fluid flow under various temperature distributions, and obtains the critical angular velocity, critical velocity of fluid flow, critical temperature changes of the structure. For the first time in the present study, mass-spring systems been considered in the rotating cylindrical thick shells conveying viscous fluid flow. The modeled cylindrical thick shell, its equations of motion, and boundary conditions are derived by the Hamilton's principle and based on RHOST. The natural frequency of the structure is investigated regarding velocity of viscous fluid flow, angular velocity, temperature changes, spring-mass systems on critical speed, critical velocity, critical temperature and natural frequency of the structure. In this study, the following main results can be achieved:

1- An increase in coefficient of the spring leads to an increase in the fundamental frequency and critical velocity of fluid flow.
2- By increasing the angular velocity, velocity of fluid flow and temperature changes, the natural frequency and stability area tends to decrease.
3- The uniform thermal distribution has the higher stability area in comparison with other thermal distributions.
4- By increasing the lumped mass and coefficient of the spring in the first frequency of the cantilever cylindrical shell, increase or decrease of the natural

frequency depends on the nonlinear temperature change parameter.

5- In the low nonlinear temperature changes, by increasing the coefficient of the spring, the natural frequency increases while by increasing the lumped mass at the free end, the natural frequency decreases.

Appendix

The parameters used in Eqs (23) and (24):

$$N_{xx}^{*}=\begin{bmatrix}\bar{Q}_{11}\left[\dfrac{\partial u_0}{\partial x}+z\dfrac{\partial u_1}{\partial x}+z^2\dfrac{\partial u_2}{\partial x}\right]+\bar{Q}_{13}\left[w_1+2zw_2\right]\\ +\bar{Q}_{12}\left[\dfrac{1}{R(1+\dfrac{z}{R})}\left(\begin{matrix}(1+\dfrac{z}{R})\dfrac{\partial v_0}{\partial\theta}+z\dfrac{\partial v_1}{\partial\theta}\\ +z^2\dfrac{\partial v_2}{\partial\theta}+w_0+zw_1+z^2w_2\end{matrix}\right)\right]\end{bmatrix}(1+z/R)$$

where parameters used in above equations are defined as:

$$\left[A_{ij}\ \ B_{ij}\ \ C_{ij}\ \ D_{ij}\ \ E_{ij}\right]=\int_{-h/2}^{h/2}\bar{Q}_{ij}\left[1\ \ z\ \ z^2\ \ z^3\ \ z^4\right]dz\,,\{i,j\}=1:6$$

$$\left[A_{ij}^{*}\ \ B_{ij}^{*}\ \ C_{ij}^{*}\ \ D_{ij}^{*}\ \ E_{ij}^{*}\right]=\int_{-h/2}^{h/2}\bar{Q}_{ij}(1+\frac{z}{R})\left[1\ \ z\ \ z^2\ \ z^3\ \ z^4\right]dz\,,\{i,j\}=1:6$$

$$\left[A_{ij}^{**}\ \ B_{ij}^{**}\ \ C_{ij}^{**}\ \ D_{ij}^{**}\ \ E_{ij}^{**}\right]=\int_{-h/2}^{h/2}\bar{Q}_{ij}(1+\frac{z}{R})^2\left[1\ \ z\ \ z^2\ \ z^3\ \ z^4\right]dz\,,\{i,j\}=1:6$$

$$\left[A_{ij}^{\otimes}\ \ B_{ij}^{\otimes}\ \ C_{ij}^{\otimes}\ \ D_{ij}^{\otimes}\ \ E_{ij}^{\otimes}\right]=\int_{-h/2}^{h/2}\frac{\bar{Q}_{ij}}{(1+\dfrac{z}{R})}\left[1\ \ z\ \ z^2\ \ z^3\ \ z^4\right]dz\,,\{i,j\}=1:6$$

References

[1] Bryan GH. (1890) On the beats in the vibrations of a revolving cylinder or bell. *Proceedings of the Cambridge Philosophical Society*. 101-111.

[2] DiTaranto R and Lessen M. (1964) Coriolis acceleration effect on the vibration of a rotating thin-walled circular cylinder. *Journal of Applied Mechanics* 31: 700-701.

[3] Srinivasan A and Lauterbach GF. (1971) Traveling waves in rotating cylindrical shells. *Journal of Engineering for Industry* 93: 1229-1232.

[4] Zohar A and Aboudi J. (1973) The free vibrations of a thin circular finite rotating cylinder. *International Journal of Mechanical Sciences* 15: 269-278.

[5] Pourmoayed A, Malekzadeh Fard K and Shahravi M. (2017) Vibration Analysis of a Cylindrical Sandwich Panel with Flexible Core Using an Improved Higher-Order Theory. *Latin American Journal of Solids and Structures* 14: 714-742.

[6] Khalili S, Davar A and Fard KM. (2012) Free vibration analysis of homogeneous isotropic circular cylindrical shells based on a new three-dimensional refined higher-order theory. *International Journal of Mechanical Sciences* 56: 1-25.

[7] Jabbari M, Nejad MZ and Ghannad M. (2015) Thermo-elastic analysis of axially functionally graded rotating thick cylindrical pressure vessels with variable thickness under mechanical loading. *International Journal of Engineering Science* 96: 1-18.

[8] Nejad MZ, Jabbari M and Ghannad M. (2015) Elastic analysis of axially functionally graded rotating thick cylinder with variable thickness under non-uniform arbitrarily pressure loading. *International Journal of Engineering Science* 89: 86-99.

[9] Afshin A, Zamani Nejad M and Dastani K. (2017) Transient thermoelastic analysis of FGM rotating thick cylindrical pressure vessels under arbitrary boundary and initial conditions. *Journal of Computational Applied Mechanics* 48: 15-26.

[10] Firouz-Abadi R, Noorian M and Haddadpour H. (2010) A fluid–structure interaction model for stability analysis of shells conveying fluid. *Journal of Fluids and Structures* 26: 747-763.

[11] Bochkarev S and Matveenko V. (2013) Numerical analysis of stability of a stationary or rotating circular cylindrical shell containing axially flowing and rotating fluid. *International Journal of Mechanical Sciences* 68: 258-269.

[12] Paak M, Païdoussis M and Misra A. (2013) Nonlinear dynamics and stability of cantilevered circular cylindrical shells conveying fluid. *Journal of Sound and Vibration* 332: 3474-3498.

[13] Rabani Bidgoli M, Saeed Karimi M and Ghorbanpour Arani A. (2016) Nonlinear vibration and instability analysis of functionally graded CNT-reinforced cylindrical shells conveying viscous fluid resting on orthotropic Pasternak medium. *Mechanics of Advanced Materials and Structures* 23: 819-831.

[14] Shahsiah R and Eslami M. (2003) Thermal buckling of functionally graded cylindrical shell. *Journal of Thermal Stresses* 26: 277-294.

[15] Mirzavand B, Eslami MR and Shahsiah R. (2005) Effect of imperfections on thermal buckling of functionally graded cylindrical shells. *AIAA journal* 43: 2073-2076.

[16] Mirzavand B and Eslami M. (2006) Thermal buckling of imperfect functionally graded cylindrical shells based on the Wan–Donnell model. *Journal of Thermal Stresses* 29: 37-55.

[17] Huang H and Han Q. (2008) Buckling of imperfect functionally graded cylindrical shells under axial compression. *European Journal of Mechanics-A/Solids* 27: 1026-1036.

[18] Banerjee J. (2012) Free vibration of beams carrying spring-mass systems− A dynamic stiffness approach. *Computers & structures* 104: 21-26.

[19] Hozhabrossadati SM, Aftabi Sani A and Mofid M. (2016a) Free vibration analysis of a beam with an intermediate sliding connection joined by a mass-spring system. *Journal of Vibration and Control* 22: 955-964.

[20] Hozhabrossadati SM, Sani AA and Mofid M. (2016b) A closed-form study on the free vibration of a grid joined by a mass-spring system. *Journal of Vibration and Control* 22: 1147-1157.

[21] Hozhabrossadati SM, Sani AA and Mofid M. (2015) Vibration of beam with elastically restrained ends and rotational spring-lumped rotary inertia system at mid-span. *International Journal of Structural Stability and Dynamics* 15: 1450040.

[22] Tauchert TR. (1974) *Energy principles in structural mechanics*: McGraw-Hill Companies.

[23] M. Rabani Bidgoli, M. Saeed Karimi, and A. Ghorbanpour Arani, "Nonlinear vibration and instability analysis of functionally graded CNT-reinforced cylindrical shells conveying viscous fluid resting on orthotropic Pasternak medium," *Mechanics of Advanced Materials and Structures,* vol. 23, pp. 819-831, 2016.

[24] SafarPour H, Hosseini M and Ghadiri M. (2017) Influence of three-parameter viscoelastic medium on vibration behavior of a cylindrical nonhomogeneous microshell in thermal environment: An exact solution. *Journal of Thermal Stresses*: 1-15.

[25] Kadoli R and Ganesan N. (2006) Buckling and free vibration analysis of functionally graded cylindrical shells subjected to a temperature-specified boundary condition. *Journal of Sound and Vibration* 289: 450-480.

[26] Shafiei N, Mirjavadi SS, Afshari BM, et al. (2017) Nonlinear thermal buckling of axially functionally graded micro and nanobeams. *Composite Structures* 168: 428-439.

[27] Zeighampour H and Beni YT. (2014) Size-dependent vibration of fluid-conveying double-walled carbon nanotubes using couple stress shell theory. *Physica E: Low-dimensional Systems and Nanostructures* 61: 28-39.

[28] Ghadiri M, Shafiei N and Safarpour H. (2016) Influence of surface effects on vibration behavior of a rotary functionally graded nanobeam based on Eringen's nonlocal elasticity. *Microsystem Technologies*: 1-21.

[29] Barooti MM, Safarpour H and Ghadiri M. (2017) Critical speed and free vibration analysis of spinning 3D single-walled carbon nanotubes resting on elastic foundations. *The European Physical Journal Plus* 132: 6.

[30] SafarPour H and Ghadiri M. (2017) Critical rotational speed, critical velocity of fluid flow and free vibration analysis of a spinning SWCNT conveying viscous fluid. *Microfluidics and Nanofluidics* 21: 22.

[31] Shu C. (2012) *Differential quadrature and its application in engineering*: Springer Science & Business Media.

[32] Civalek Ö. (2004) Application of differential quadrature (DQ) and harmonic differential quadrature (HDQ) for buckling analysis of thin isotropic plates and elastic columns. *Engineering Structures* 26: 171-186.

[33] Mirsky I and Herrmann G. (1957) Nonaxially symmetric motions of cylindrical shells. *The Journal of the Acoustical Society of America* 29: 1116-1123.

[34] Reddy J. (1984) Exact solutions of moderately thick laminated shells. *Journal of Engineering Mechanics* 110: 794-809.

[35] Armenàkas AE, Gazis DC and Herrmann G. (2016) *Free vibrations of circular cylindrical shells*: Elsevier.

[36] Loy C and Lam K. (1999) Vibration of thick cylindrical shells on the basis of three-dimensional theory of elasticity. *Journal of Sound and Vibration* 226: 719-737.

[37] Loy C, Lam K and Shu C. (1997) Analysis of cylindrical shells using generalized differential quadrature. *Shock and Vibration* 4: 193-198.